J. Fluid Mech. (1992), *vol.* 238, *pp.* 699–722
Printed in Great Britain

Scaling of adverse-pressure-gradient turbulent boundary layers

By P. A. DURBIN AND S. E. BELCHER
Center for Turbulence Research, Stanford University, Stanford, CA 94305-3030, USA

(Received 4 March 1991 and in revised form 27 September 1991)

An asymptotic analysis is developed for turbulent boundary layers in strong adverse pressure gradients. It is found that the boundary layer divides into three distinguishable regions: these are the wall layer, the wake layer and a transition layer. This structure has two key differences from the zero-pressure-gradient boundary layer: the wall layer is not exponentially thinner than the wake; and the wake has a large velocity deficit, and cannot be linearized. The mean velocity profile has a $y^{\frac{1}{2}}$ behaviour in the overlap layer between the wall and transition regions.

The analysis is done in the context of eddy viscosity closure modelling. It is found that k–ε-type models are suitable to the wall region, and have a power-law solution in the $y^{\frac{1}{2}}$ layer. The outer-region scaling precludes the usual ε-equation. The Clauser, constant-viscosity model is used in that region. An asymptotic expansion of the mean flow and matching between the three regions is carried out in order to determine the relation between skin friction and pressure gradient. Numerical calculations are done for self-similar flow. It is found that the surface shear stress is a double-valued function of the pressure gradient in a small range of pressure gradients.

1. Introduction

The adverse-pressure-gradient (APG) boundary layer is of fundamental interest because it precedes separation. One must understand how a strong adverse pressure gradient distorts the boundary layer before one can address the extremely challenging problem of turbulent separation. The APG boundary layer is also of interest in its own right: even if the boundary layer does not separate, the adverse pressure can affect transport properties and skin friction. The asymptotic structure of APG turbulent boundary layers has not previously been investigated, notwithstanding the fact that much is known experimentally and theoretically about such flows. Asymptotic methods provide a systematic framework which can contribute to our understanding of turbulent boundary layers.

The scaling laws for zero-pressure-gradient (ZPG) boundary layers have been known for some time. Formal asymptotic developments were given by Yajnik (1970), Mellor (1972) and Bush & Fendell (1972); they showed how the law of the wall and law of the wake can be viewed as asymptotically distinguished regions, with the log-layer their common overlap. When a turbulent boundary layer is subject to a substantial adverse pressure gradient this two-region structure no longer applies.

In the present paper, it is shown that the APG boundary layer requires three regions to describe its asymptotic structure (figure 1). At the outset of the present investigation it was supposed that the Yajnik–Mellor scaling could be modified such

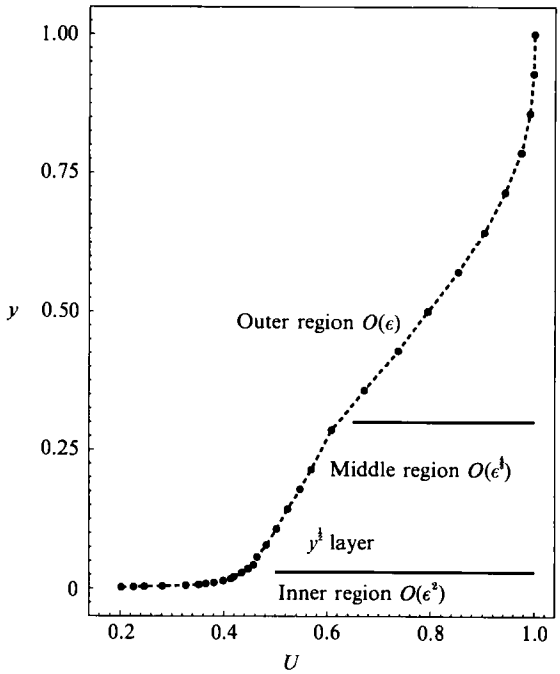

FIGURE 1. Mean flow profile for APG boundary layer, showing the three-region structure. Experimental data is by Bradshaw and Ferris (Coles & Hirst 1968).

that a $y^{\frac{1}{2}}$ layer would replace the log-layer: a $y^{\frac{1}{2}}$ layer is expected on theoretical and experimental grounds (Townsend 1976; Perry & Schofield 1973). However, the wall and wake regions did not overlap in such a layer: an intermediate region was needed. The intermediate region does overlap the wall region in a $y^{\frac{1}{2}}$ layer on one side, and also matches to the wake region on the other side. Thus, the three-layer structure arises out of mathematical requirements of the asymptotic analysis. On examination of this analysis, it becomes apparent that the intermediate layer exists to allow the turbulent transport processes to make a transition from their near-wall behaviour to their wake-region behaviour. The three-layer structure is consistent with the peak turbulent kinetic energy being located well away from the wall, which is a known property of APG turbulent boundary layers.

In the ZPG boundary layer the wake velocity deficit is small, and the mean wake velocity is uniform to leading order. The only way the thin wall layer can match to this constant wake velocity is for the overlap law to be logarithmic and for the perturbation parameter to vary inversely as the logarithm of the Reynolds number (Mellor 1972); this is simply a statement of Millikan's overlap argument in formal asymptotic terms. The structure of ZPG boundary layers is a consequence of the fullness of the mean velocity profile; the velocity increases rapidly across a thin layer near the wall, then approaches the free-stream velocity more gradually across a thick outer region. By contrast, the APG boundary-layer profile may have an initially steep rise near the wall, but it is then eaten away by pressure gradient, so that it has a large wake deficit (figure 1). In fact, profiles of equilibrium APG layers have almost a double boundary-layer form, with an initial upturn in the $y^{\frac{1}{2}}$ region, followed by a slight flattening, with a second upturn in the outer region. The wake profile is not full, and the mean momentum equation in the wake region is fully nonlinear. The large wake deficit of APG layers invalidates the 'Millikan overlap' derivation of the

log-law. In the presence of a strong APG, matching must take place in regions where the mean velocity varies as a power of y. This is a primary analytical distinction between APG and ZPG boundary layers. The asymptotic structure of APG layers is described in §2.

The three asymptotic regions of an APG turbulent boundary layer reflect three velocity scales which exist in such a flow. They are: the viscous, pressure-gradient velocity, defined in §2; the free-stream velocity; and the square-root of the boundary layer thickness times kinematic pressure gradient. The first is used to non-dimensionalize the mean velocity in the wall region, the second non-dimensionalizes the wake region, and the last non-dimensionalizes the middle region. Another velocity scale is the friction velocity. In the present analysis this is taken to be of the same order as the viscous, pressure-gradient velocity.

The structure of attached turbulent boundary layers is more complex than that of laminar layers. This is because turbulent transport is a property of the flow, while viscous transport is a constitutive property. As the pressure gradient alters the mean flow, so will the turbulent transport processes alter; this effect does not occur in laminar layers. Some conception of the behaviour of turbulent transport is required if one is to address the issue of strongly APG boundary layers. Closure models provide a basis for such conceptions and, conversely, the asymptotic analysis of the structure of the boundary layer provides some guidance to the development of closure models (Mellor 1972). Bush & Fendell (1972) and Melnik (1989, 1991) have applied asymptotic methods to analyses of algebraic eddy viscosity models. Here we use algebraic and k–ε-types of eddy viscosity models. The relevance of the present analysis to the development of such models will be discussed. As usual, much of the present analysis could be developed in a more general setting, but models are needed to obtain specific results, so we have chosen to introduce an eddy viscosity assumption at the outset. However, this emphasis on turbulence models should not detract from the fundamental nature of the present analysis; its relevance is by no means restricted to the particular models being considered.

Our analysis highlights some important properties of the k–ε eddy viscosity model. The k–ε equations are found to have a power-law solution in the $y^{\frac{1}{3}}$ layer. This is analogous to their solution in the log layer of the ZPG boundary layers. The power-law solution is derived in §3. Given the standard model constants, the solution for k (the turbulent kinetic energy) and ε (its rate of dissipation) is then completely determined. Although the k–ε model is fundamentally unsuitable near solid boundaries, the k–ε–v model (Durbin 1991), which accounts for wall blocking and anisotropy of the eddy viscosity, has a similar power-law solution.

The usual ε-equation appears to be inappropriate in the wake region of turbulent boundary layers; in the present paper, it is found to be inconsistent with the wake region scaling. The Clauser, constant eddy viscosity (Clauser 1956) is a popular model for this region. That model will be used here. Because the k–ε model does not give proper wake region scaling, a transition between the k–ε (or k–ε–v) model for the wall layer and the Clauser model for the wake region must occur across the middle layer. In the middle region k increases linearly, at a rate determined by matching to the wall region. Given this result, the energy equation can then be used as a basis for arriving at a formula for the transition between the wall and wake transport models – the ε-equation is not needed.

In order to determine the skin friction law, the complete problem of matched asymptotic expansions must be considered, since ultimately it is the free-stream velocity which produces the skin friction at the surface. In order to determine the

effect of the free stream at the surface, the transport of mean momentum across the boundary layer must be determined, and this requires that the asymptotic matching be considered. From the scaling alone, one finds that the ratio of viscous, pressure-gradient velocity to free-stream velocity is of order Reynolds number to the $-\frac{1}{3}$ (equation (2.2)). In the present analysis the friction velocity is assumed to be of the same order of magnitude. Although a $-\frac{1}{3}$ power friction law is then true by assumption, it is significant that this gives a consistent asymptotic picture. The matching problem is addressed in §4.

The specific case of self-preserving development is addressed in §4.2. This requires that the Falkner–Skan equation can be solved in the outer region, with boundary conditions determined by the inner regions. Our numerical results show that when the APG is small, the non-dimensional skin friction decreases with increasingly adverse pressure gradient, as one might expect. However, as the skin friction tends toward zero, the pressure gradient goes through a broad maximum, so that there is a small range in which two equilibrium boundary layers exist for a given pressure gradient. Remarkably, this surprising theoretical result agrees with an observation made some time ago by Clauser (1954) in an analysis of his experimental data. Since the pioneering paper by Clauser, the existence of multivalued equilibrium boundary layers has been debated: at present the bulk of experimental evidence concurs with Clauser's observation (Schofield 1981). In the present theoretical derivation, the doubled-valued solution arises from the asymptotic matching conditions and from properties of the Falkner–Skan equation.

2. Scaling of the regions

We consider a uniform-density, incompressible turbulent boundary layer subject to a strong adverse pressure gradient (APG) – a criterion for the adjective 'strong' is developed in §2.5. The free-stream mean velocity is $U_\infty(x)$. We define the kinematic pressure gradient α, streamwise lengthscale L and viscous pressure-gradient velocity u_p by

$$\alpha \equiv -U_\infty U_{\infty x}; \quad L \equiv U_\infty^2/\alpha; \quad u_p \equiv (\nu\alpha)^{\frac{1}{3}}. \tag{2.1}$$

The definition of u_p reflects the fact that the relevant dimensional parameters near the wall are ν (the kinematic viscosity) and α. The small parameter in the present analysis is

$$\epsilon \equiv u_p/U_\infty = (\nu\alpha/U_\infty^3)^{\frac{1}{3}} = R_L^{-\frac{1}{3}}, \tag{2.2}$$

where R_L is the Reynolds number based on L. In general δ/L, where δ is a measure of the boundary-layer thickness, is another small parameter. In the present analysis it is sufficient, although not necessary, to let $\delta/L \sim \epsilon$; this gives the appropriate leading-order balance between pressure gradient and turbulence shear stress gradient in the middle and outer regions. Given this ordering, one can define δ such that this latter relation is an equality. In most of the analysis it is appropriate to think of δ/L as the small parameter. The middle and outer regions are inviscid to lowest order, so it would be misleading to associate the small parameter with Reynolds number in these regions; perhaps (2.2) should be expressed as $R_L = \epsilon^{-3}$.

2.1. *The inner region*

The mean flow profile is illustrated by figure 1. The inner, wall region lies closest to the surface and extends from the surface to the $y^{\frac{1}{2}}$ layer. According to the information given by Coles & Hirst (1968), in which the data plotted in figure 1 are tabulated,

$u_p = 0.22$ m/s, $u_* = 1.1$ m/s, $U_\infty = 41$ m/s, $L = 2.28$ m and $\delta_{0.99} = 3$ cm for these data. This gives $\epsilon \approx 0.005$. According to figure 1, the inner region is $O(\epsilon)$ smaller than the overall boundary-layer thickness, and so consists only of the region next to the surface, in which U rises steeply. The non-dimensional variables in the inner region are distinguished by a hat:

$$\hat{y} = yu_p/\nu; \quad \hat{U} = U/u_p; \quad \hat{\nu}_T = \nu_T/\nu; \quad \hat{k} = k/u_p^2; \quad \hat{\varepsilon} = \varepsilon\nu/u_p^4. \tag{2.3}$$

The lengthscale here is $\nu/u_p = \epsilon^2 L$. u_p is used for the velocity scale in the inner region. The friction velocity u_* is inappropriate because it can tend to zero in APG boundary layers. In (2.3) ν_T is the eddy viscosity, k is the turbulent kinetic energy and ε is the rate of energy dissipation.

An eddy viscosity model for the Reynolds shear stress will be introduced at the outset. Thus, the mean momentum and continuity equations in the boundary layer are

$$UU_x + VU_y + \alpha = ((\nu + \nu_T)\, U_y)_y, \qquad U_x + V_y = 0, \tag{2.4}$$

where ν_T is the turbulent eddy viscosity and in which lower-case subscripts denote partial differentiation. In the wall region, the k–ε eddy viscosity formula, $\nu_T = C_\mu k^2/\varepsilon$, gives the behaviour of ν_T. In principle, C_μ is a constant; in practice, C_μ is made a function of y, to account for 'wall damping' (Patel, Rodi & Scheurer 1985). (It is more fundamentally sound to use the formula $\nu_T = C_\mu k\overline{v^2}/\varepsilon$, with C_μ now being constant (Durbin 1991). However, the k–ε formula suffices for the purpose of getting the scaling.) The k–ε model is discussed in §3.

In terms of the non-dimensional variables introduced in (2.3), equation (2.4) simplifies to

$$((1 + \hat{\nu}_T)\, \hat{U}_{\hat{y}})_{\hat{y}} = 1 + O(\epsilon^2) \tag{2.5}$$

in the inner region. If the friction velocity u_* is defined by $u_*^2 = \nu U_y$ at $y = 0$, then (2.5) integrates to

$$(1 + \hat{\nu}_T)\, \hat{U}_{\hat{y}} = \hat{y} + \frac{u_*^2}{u_p^2} + O(\epsilon^2) \tag{2.6}$$

because $\hat{\nu}_T = 0$ at $\hat{y} = 0$. Present interest is in an APG that is sufficiently strong for u_*/u_p to be of $O(1)$.

The no-slip boundary condition to (2.6) is $\hat{U} = 0$ at $y = 0$. On general, semi-empirical grounds, one expects that as $\hat{y} \to \infty$, $\hat{U} \to A_u \hat{y}^{\frac{1}{2}}$. Townsend (1976, eq. 5.14.9), following earlier work of Stratford, derives the half-power law from a mixing-length model. It is shown in §3 that the k–ε model also has this solution, with the standard model constants giving $A_u = 7.65$. Experimental data in self-preserving APG flow also contain half-power layers.

2.2. *The need for a middle region*

A middle region is required fundamentally because if the wall region were to match with the wake region, then the boundary-layer approximation, $\delta/L \sim \epsilon$, would be contradicted. The reasoning is as follows: suppose that the inner region with the scaling (2.3) were to overlap with an outer region in which $y = O(\delta)$. Then in the $y^{\frac{1}{2}}$ overlap layer the mean velocity determined by (2.3) would be of order $u_p(\delta u_p/\nu)^{\frac{1}{2}}$. The outer region velocity scale is determined by the condition at infinity, and so is of order U_∞. Overlap of the regions could occur only if

$$U_\infty \sim u_p(\delta u_p/\nu)^{\frac{1}{2}} = U_\infty\, O(\delta/L)^{\frac{1}{2}}.$$

Hence the supposed overlap leads to the contradiction $\delta \sim L$. In the present analysis $\delta/L \sim \epsilon$ has been assumed, although in general it is necessary only that

$$1 \gg \delta/L \gg \epsilon^2.$$

One can conclude that the APG velocity profile is not analogous to that of ZPG boundary layers – that analogy is often assumed. Similarly, it is inconsistent with the boundary-layer approximation to deduce a drag law by borrowing Millikan's argument, as was done by Yaglom (1979).

A middle region must be introduced in order to match the inner and outer regions. In this region y is $O(\delta\gamma)$ where $\gamma \ll 1$. In the present case, where $\delta/L = \epsilon$, γ can be ϵ to any power p which satisfies $0 < p < 1$. In §2.4 it is explained that $\gamma = \epsilon^{\frac{1}{3}}$ is the power which matches to the constant eddy viscosity of Clauser (1956) in the outer region. In the present paper this $\frac{1}{3}$ power will be used – it is the scaling shown in figure 1. If instead, the outer region were modelled with a constant mixing length (Bradshaw 1967) then $\gamma = \epsilon^{\frac{1}{2}}$ would be appropriate.

2.3. *The middle region*

The lengthscale in the middle region is $\delta\gamma$. The velocity scale, which follows from this lengthscale and matching to the $y^{\frac{1}{2}}$ layer, is $(\alpha\delta\gamma)^{\frac{1}{2}}$. With the choice for γ just described, these are equivalent to $\delta\epsilon^{\frac{1}{3}}$ and $U_\infty \epsilon^{\frac{2}{3}}$. Although this latter form will be used, it should be appreciated that the middle-region velocity scale is determined by the pressure gradient and boundary-layer thickness: it is not U_∞. In the data of figure 1, $\epsilon^{\frac{1}{3}} \approx 0.17$. This is the fraction of the boundary layer occupied by the middle region. Hence, the middle region is the portion of the profile in which $\mathrm{d}U/\mathrm{d}y$ has decreased greatly from its near-wall level, and the profile turns upward.

The non-dimensional variables in the middle region are distinguished by an overbar:

$$\bar{y} = \frac{y}{\delta\epsilon^{\frac{1}{3}}}; \quad \bar{U} = \frac{U}{U_\infty \epsilon^{\frac{2}{3}}}; \quad \bar{\nu}_\mathrm{T} = \frac{\nu_\mathrm{T}}{U_\infty \delta\epsilon}; \quad \bar{k} = \frac{k}{U_\infty^2 \epsilon^{\frac{4}{3}}}; \quad \bar{\varepsilon} = \frac{\varepsilon}{U_\infty^3 \epsilon^{\frac{2}{3}}/L}. \tag{2.7}$$

The lengthscale here is $\epsilon^{\frac{4}{3}}L$, with the present identification of δ/L and ϵ. The normalization of ν_T follows from matching with the eddy viscosity used in the outer, wake region. The scaling of k and ε in (2.7) was determined from the required overlap with the wall region in the $y^{\frac{1}{2}}$ layer – see (3.4).

The equation governing the mean flow in the middle region follows from (2.4) and (2.7); it is

$$(\bar{\nu}_\mathrm{T}\, \bar{U}_{\bar{y}})_{\bar{y}} = 1 + O(\epsilon^{\frac{4}{3}}). \tag{2.8}$$

As $\bar{y} \to 0$ this will match to the $y^{\frac{1}{2}}$ layer; as $\bar{y} \to \infty$, we assume that $\bar{\nu}_\mathrm{T}$ tends to a constant, so $\bar{U}$ goes as $\bar{y}^2$.

The standard k–ε model (see §3) does not admit a power-law solution with $\bar{U}$ going as $\bar{y}^2$. Hence the eddy viscosity in the middle region cannot be described by this model. The middle-region viscosity must interpolate between the k–ε-type of viscosity, which is valid in the inner region, and the constant Clauser viscosity, which is valid in the outer region. This will be discussed in §3.2. At present we simply note that, given an eddy viscosity profile, (2.8) determines the mean flow profile in the middle region. To lowest order it is

$$\bar{U} = \int_0^{\bar{y}} \frac{\bar{y}\,\mathrm{d}\bar{y}}{\bar{\nu}_\mathrm{T}}. \tag{2.9}$$

2.4. *The outer region*

The APG boundary layer has a large velocity deficit in its wake region. Hence, the mean momentum equation in the outer region cannot be linearized. The non-dimensional variables in the outer region are distinguished by a tilde:

$$\tilde{y} = \frac{y}{\delta}; \quad \mathrm{d}\tilde{x} = \frac{\mathrm{d}x}{L}; \quad \tilde{U} = \frac{U}{U_\infty}; \quad \tilde{V} = \frac{V}{U_\infty \epsilon}; \quad \tilde{\nu}_\mathrm{T} = \frac{\nu_\mathrm{T}}{U_\infty \delta \epsilon}; \quad \tilde{k} = \frac{k}{U_\infty^2 \epsilon}; \quad \tilde{\varepsilon} = \frac{\varepsilon}{U_\infty^3/L}. \tag{2.10}$$

Note that with the present identification of ϵ and δ/L, the factor normalizing the eddy viscosity is equal to $U_\infty \delta^2/L$. This is the scaling required in the nonlinear wake region; by contrast, in the ZPG wake deficit law the eddy viscosity is normalized by $u_* \delta^2/L$, and the mean momentum equation can be linearized (Mellor 1972). k and ε do not play a role in the outer region because the Clauser viscosity (see (3.13)) is adopted; they are included in (2.10) to show that k matches to a linear profile when $\tilde{y} \to 0$, which fact will be used in §3.2, and to show how ε varies across the boundary layer. The scaling for ε is found by assuming that it is the same as that for production:

$$\mathscr{P} = \nu_\mathrm{T} U_y^2 \sim (\epsilon \delta U_\infty)(U_\infty/\delta)^2 \sim U_\infty^3/L.$$

The scaling for k comes from the order of magnitude estimate $k^2/\varepsilon \sim \nu_\mathrm{T}$.

The mean momentum equation (2.4) becomes

$$\tilde{U}\tilde{U}_{\tilde{x}} + \tilde{V}\tilde{U}_{\tilde{y}} - \tilde{y}\tilde{U}\tilde{U}_{\tilde{y}}\,\delta_{\tilde{x}}/\delta - \tilde{U}^2 + 1 = (\tilde{\nu}_\mathrm{T}\tilde{U}_{\tilde{y}})_{\tilde{y}} \tag{2.11}$$

in the outer, wake region. Here we have allowed for an $\tilde{x}$-dependence of U_∞ and δ. The definition of L is that $\partial_{\tilde{x}} U_\infty = -U_\infty$ (see (2.1)); this was used in the derivation of (2.11). $\tilde{V}$ is determined by the continuity equation:

$$\tilde{U}_{\tilde{x}} + \tilde{V}_{\tilde{y}} - \tilde{U} - (\delta_{\tilde{x}}/\delta)\,\tilde{y}\tilde{U}_{\tilde{y}} = 0.$$

In the overlap layer between the middle and outer regions the scaling leads to power-law dependence. Writing the middle region functions (2.7) in outer variables and requiring that they match independently of ϵ to the outer functions (2.10) implies

$$\bar{U} \to O(\bar{y}^2); \quad \bar{k} \to O(\bar{y}); \quad \bar{\varepsilon} \to O(\bar{y}^2); \quad \bar{\nu}_\mathrm{T} \to O(1). \tag{2.12}$$

The behaviour of $\bar{\nu}_\mathrm{T}$ is by construction: we have let $\gamma = \epsilon^{\frac{1}{3}}$ in the middle region in order to obtain a constant viscosity in the outer region; the $\bar{y}^2$ form of $\bar{U}$ is a consequence. If $\bar{U}$ were to be $O(\bar{y}^n)$ then γ would have to be $O(\epsilon^{1/(2n-1)})$. The relative size of the middle region in figure 1 would then be $O(\epsilon^{2n/(2n-1)})$. If instead of requiring that the eddy viscosity be constant in the outer region, one required the Prandtl mixing length, defined as $(\nu_\mathrm{T}/U_y)^{\frac{1}{2}}$, to be constant, then n would be $\frac{3}{2}$.

2.5. *Discussion*

Consider a boundary layer starting in a small pressure gradient and developing into a region of increasingly adverse pressure gradient. Upstream the ZPG structure of Yajnik (1970) and Mellor (1972) is appropriate. Far downstream the present structure applies. The transition between these structures takes place as the log-layer becomes submerged below a $y^{\frac{1}{2}}$ layer. The present scaling does not reduce to the ZPG scaling when $u_p \to 0$, nor does the ZPG scaling reduce to the present scaling when

$u_* \to 0$. A model for the near-wall region, such as that given by Townsend (1976, eq. 5.15.3), is needed to interpolate between the ZPG and APG regions. His equation has the correct $y^{\frac{1}{2}}$ behaviour when $u_*/u_p \to 0$ and logarithmic behaviour when $u_p/u_* \to 0$. Hence it provides a formula for an intermediate region when $u_p/u_* \sim 1$.

The transition from a log-layer to a half-power layer reflects the change of the wall region from a layer of constant stress to one of linearly varying stress. That observation may be used to develop a criterion for the validity of the present analysis. The shear stress in the overlap layer between the wall and transition regions is given by

$$\tau = \alpha y + u_*^2. \tag{2.13}$$

Since the lengthscales of the wall and transition regions are respectively $\epsilon^2 L$ and $\epsilon\gamma L = \epsilon^{\frac{4}{3}} L$, an intermediate lengthscale for the overlap layer is $l = \epsilon^{m+1} L$, with $\frac{1}{3} < m < 1$. The present scaling requires that in the overlap layer the first term on the right-hand side of (2.13) be large compared to the second: $\alpha l \gg u_*^2$. This inequality must be satisfied in order to obtain a $y^{\frac{1}{2}}$ layer. Using the estimate for l and the definition of u_p, the inequality can be written $\epsilon^{1-m} u_*^2/u_p^2 \ll 1$, so another way to state the condition for the validity of the present scaling is

$$\epsilon\, u_*^2/u_p^2 \ll \epsilon^m \ll 1. \tag{2.14}$$

Using $\delta/L \sim u_p/U_\infty \sim \epsilon$ this can also be written as a criterion for the magnitude of the pressure gradient:

$$L/\delta \ll U_\infty^2/u_*^2. \tag{2.15}$$

Although this is a statement that L be sufficiently small, the right-hand side of this equation is asymptotically large at high Reynolds number – the precise scaling depends on the drag law – hence, the present approximations are valid when the lengthscale of the pressure gradient is still large compared to the boundary-layer thickness. Recall that L varies inversely with the pressure gradient, so $L \to \infty$ as the pressure gradient tends to zero. Then, according to (2.15) the present scaling becomes valid only when L has been reduced; that is, when the pressure gradient has become sufficiently large.

A number of important conclusions can be drawn from the scaling provided here. One is that a strong adverse pressure gradient applied to a ZPG boundary layer will cause the law-of-the-wall region to split into a wall region and a transition region, because the APG boundary layer has a large deficit wake that cannot match directly to the wall region. If u_* is not small compared to u_p, then a log-layer can be distinguished within the present wall region. To the extent that a log-layer can be distinguished, it lies below the $y^{\frac{1}{2}}$ layer (Townsend 1976).

Another noteworthy feature of the present scaling is the predicted behaviour of ε: in the inner region ε is $O(\epsilon)$, when normalized by U_∞^3/L; in the middle region it is $O(\epsilon^{\frac{4}{3}})$; and in the outer region it is $O(1)$. This result is rather unexpected because in the ZPG boundary layer ε has a sharp peak at the wall and decreases montonically away from the wall. The present result that ε increases away from the wall in APG boundary layers seems a bit surprising. The experimental evidence of Bradshaw (1967) is not entirely conclusive, but it shows convincingly that ε is large in the outer region of APG boundary layers, in striking contrast to the ZPG case.

The scaling for k/U_∞^2 shows it to increase from $O(\epsilon^2)$ to $O(\epsilon^{\frac{4}{3}})$ to $O(\epsilon)$, moving away from the wall. Again, this contrasts to the ZPG case, for which k decreases greatly from the inner region to the outer region. This scaling for k agrees qualitatively with experimental trends (Bradshaw 1967).

The present scaling also shows that in the outer region the lowest-order balance in the turbulent kinetic energy equation is between production and dissipation; the transport terms are formally of $O(\epsilon)$ smaller. In the ZPG boundary layer the transport term is formally of the same order as production and dissipation. The difference between the cases of zero and adverse pressure gradient is the mean shear, and hence the rate of production of turbulent kinetic energy, is much larger in the latter. A corollary to the present scaling is that the standard ε-equation (see §3) cannot be satisfied in the outer region: the transport term in the ε-equation cannot balance production and dissipation of ε, nor can these latter two terms balance each other in the conventional model (see (3.1)). Hence, the standard k–ε model is inconsistent with the scaling of the outer region of APG turbulent boundary layers.

3. Turbulence modelling

The previous analysis suggests that one might solve the k–ε model equations in the half-power, linear stress layer. This is done here. This solution is then used to propose an interpolation formula for the eddy viscosity in the middle layer. The interpolation formula is needed in order to obtain the matching conditions required in §4 to solve the outer-region momentum equations.

3.1. *The k–ε model in the $y^{\frac{1}{2}}$ layer*

The $y^{\frac{1}{2}}$-layer in APG boundary layers assumes the role which the log-layer plays in ZPG boundary layers. This layer corresponds to the simultaneous limits $\hat{y}\to\infty$ and $\bar{y}\to 0$. Just as the k–ε model has a simple solution in the log-layer, so it has in the $y^{\frac{1}{2}}$ layer.

The standard k–ε equations (Patel *et al.* 1985) in the steady-state limit, which is suitable to the order of approximation of the wall layer, are

$$\left(\frac{\hat{\nu}_{\mathrm{T}}}{\sigma_k}\hat{k}_{\hat{y}}\right)_{\hat{y}} = \hat{\varepsilon}-\hat{\nu}_{\mathrm{T}}(\hat{U}_{\hat{y}})^2, \qquad \left(\frac{\hat{\nu}_{\mathrm{T}}}{\sigma_e}\hat{\varepsilon}_{\hat{y}}\right)_{\hat{y}} = \frac{C_{\varepsilon_2}\hat{\varepsilon}-C_{\varepsilon_1}\hat{\nu}_{\mathrm{T}}(\hat{U}_{\hat{y}})^2}{\hat{k}/\hat{\varepsilon}} \tag{3.1}$$

where C_{ε_1} and C_{ε_2} are constants and σ_k and σ_e are Prandtl numbers for the transport of kinetic energy and its dissipation respectively. The eddy viscosity is given by

$$\hat{\nu}_{\mathrm{T}} = C_\mu \hat{k}^2/\hat{\varepsilon}. \tag{3.2}$$

In the $y^{\frac{1}{2}}$ layer, or from (2.6) at large $\hat{y}$,

$$\hat{U}_{\hat{y}} = \hat{y}/\hat{\nu}_{\mathrm{T}}. \tag{3.3}$$

A power-law solution in the form $\hat{U} = A_u \hat{y}^n$ is sought. Equations (3.1) and (3.3) then require that

$$\hat{\nu}_{\mathrm{T}} = A_\nu \hat{y}^{2-n}; \quad \hat{\varepsilon} = A_\varepsilon \hat{y}^n; \quad \hat{k} = A_k \hat{y}^{2n}, \tag{3.4}$$

where the A are constants. The formula (3.2) can only be satisfied if $n = \frac{1}{2}$; this is the only power law consistent with the k–ε model in a linear stress layer.

After substitution of (3.4) into (3.1), (3.2) and (3.3) the A can be found. They are given by

$$A_k = \frac{A_u^2(C_{\varepsilon_2}-C_{\varepsilon_1})\sigma_k\sigma_e}{2(\sigma_k-3\sigma_e C_{\varepsilon_2})}, \qquad A_\varepsilon = \frac{A_u(\sigma_k-3C_{\varepsilon_1}\sigma_e)}{2(\sigma_k-3\sigma_e C_{\varepsilon_2})} \tag{3.5}$$

where $$A_u^4 = \frac{4(\sigma_k - 3C_{\varepsilon_1}\sigma_e)(\sigma_k - 3C_{\varepsilon_2}\sigma_e)}{C_\mu \sigma_k^2 \sigma_\varepsilon^2 (C_{\varepsilon_2} - C_{\varepsilon_1})^2}.$$

This solution can be evaluated after substituting values for the model constants. Commonly used values are (Patel *et al.* 1985)

$$C_{\varepsilon_1} = 1.44; \quad C_{\varepsilon_2} = 1.92; \quad C_\mu = 0.09; \quad \sigma_k = 1.0; \quad \sigma_e = 1.3.$$

With these values, (3.5) gives

$$A_u = 7.65; \quad A_\varepsilon = 5.37; \quad A_k = 3.95 \tag{3.6}$$

and from (3.2) $A_\nu = 0.26$. Rather similar values are obtained from the k–ε–v model of Durbin (1991); for example, it gives $A_k = 4.02$ and $A_u = 6.75$. The similarity of these models in the $y^{\frac{1}{2}}$ layer is important because the k–ε model does not behave correctly near to walls.

Yaglom (1979) reviews analyses by himself and Kader of various experimental data on APG boundary layers. In terms of their non-dimensional variable Z, Yaglom and Kader find

$$k \approx 1.2u_*^2 Z, \quad -\overline{uv} \approx 0.25u_*^2 Z, \quad U \approx 4.5u_* Z^{\frac{1}{2}} \tag{3.7}$$

in the half-power region. Yaglom uses z as the direction normal to the wall and defines Z as $\alpha z/u_*^2$. It is not clear why the constant in the expression for $-\overline{uv}$ is not unity. In the present analysis (see (3.2)) $-\overline{uv} = \hat{y}$, so A_k is equal to $-k/\overline{uv}$. If an experimental value for A_k is evaluated by forming this ratio, then (3.7) gives it to be $A_k = 4.8$. A_u might similarly be evaluated as $U/(-\overline{uv})^{\frac{1}{2}}$. The data in (3.7) then give $A_u = 9.0$. Unfortunately the mean flow and Reynolds stress data cited by Yaglom are from different experiments, so it is not clear that this evaluation of A_u is valid. The alternative is simply to accept the value of $A_u = 4.5$ given in (3.7). In either case, there is rough agreement between the k–ε model with standard constants and the experimental data.

In practice it is often found that the shear stress gradient in the half-power region is less than the pressure gradient. To fit experimental data α must be replaced by an 'effective pressure gradient' (McDonald 1969). The failure to do this could be a source of scatter in the data considered by Yaglom. Townsend (1976) proposes that α be obtained by adding an average of the inertia term to the pressure gradient; Melnik (1989) introduces a slip velocity, which adds a term to the pressure gradient in the inner region. The empirical need for an 'effective pressure gradient' may reflect the fact that the $y^{\frac{1}{2}}$ region is not extremely thin.

3.2. *Middle-region eddy viscosity*

In the analysis of the $y^{\frac{1}{2}}$ layer given in §3.1, it was found that as $\bar{y} \to 0$ the turbulent kinetic energy tends to $\bar{k} = A_k \bar{y}$, where $A_k = 3.95$ if the standard k–ε constants are used. Matching the mean velocity to the y^2 asymptote of the outer region shows that k again increases linearly with $\bar{y}$ (see (2.12)). It seems that $\bar{k} = A_k \bar{y}$ throughout the middle layer. Another justification for this linear increase of k is that the Reynolds shear stress increases linearly in the middle region, and the kinetic energy might be expected to behave similarly.

The turbulent kinetic energy equation in the middle region is given to leading order by

$$\bar{\varepsilon} = \bar{\mathscr{P}} + \left(\frac{\bar{\nu}_T}{\sigma_k}\bar{k}_{\bar{y}}\right)_{\bar{y}}, \tag{3.8}$$

in which turbulent transport is modelled by an eddy viscosity, σ_k is a Prandtl number for this transport, and $\bar{\mathscr{P}}$ represents the rate of energy production:

$$\bar{\mathscr{P}} = -\overline{uv}\bar{U}_{\bar{y}} = \bar{\nu}_{\mathrm{T}}(\bar{U}_{\bar{y}})^2. \tag{3.9}$$

Equation (3.8) expresses a balance between dissipation, production and turbulent transport of turbulent kinetic energy. The first integral of the mean momentum equation (2.8) is $\bar{\nu}_{\mathrm{T}}\bar{U}_{\bar{y}} = \bar{y} + O(\epsilon^{\frac{3}{2}})$. Substitution of this into (3.9) shows that $\bar{\nu}_{\mathrm{T}}\bar{\mathscr{P}} = \bar{y}^2$. Using this and $\bar{k} = A_k\bar{y}$ in (3.8) gives

$$\bar{\nu}_{\mathrm{T}}\bar{\varepsilon} = \bar{y}^2 + \frac{A_k}{2\sigma_k}\partial_{\bar{y}}\bar{\nu}_{\mathrm{T}}^2. \tag{3.10}$$

As in the k–ε eddy viscosity formula given below (2.4), we let $\bar{\varepsilon} = C_\mu(\bar{y})\bar{k}^2/\bar{\nu}_{\mathrm{T}}$ (although in this case the $\bar{y}$-dependence is not associated with 'wall damping'). Then (3.10) becomes

$$(C_\mu A_k^2 - 1)\bar{y}^2 = \frac{A_k}{2\sigma_k}\partial_{\bar{y}}\bar{\nu}_{\mathrm{T}}^2. \tag{3.11}$$

The standard k–ε model uses $C_\mu = 0.09$, $\sigma_k = 1.0$ and gives $A_k = 3.95$. When substituted into (3.11) this gives the $y^{\frac{3}{2}}$ behaviour for ν_{T} that is appropriate to the $y^{\frac{1}{2}}$ layer. Matching to the constant viscosity in the outer region requires that

$$C_\mu = 1/A_k^2 \approx 0.064.$$

Thus, one might view the middle layer as a region across which C_μ decreases from 0.09 to 0.064.

This transition might be accomplished by the *ad hoc* interpolation

$$C_\mu = 1/A_k^2 + (0.09 - 1/A_k^2)\,\mathrm{e}^{-\bar{y}/\bar{d}} = 0.064 + 0.026\,\mathrm{e}^{-\bar{y}/\bar{d}}.$$

Then, integrating (3.11)

$$\begin{aligned}\bar{\nu}_{\mathrm{T}}^2 &= \frac{2}{A_k}(0.09A_k^2 - 1)\int_0^{\bar{y}} \bar{y}^2\,\mathrm{e}^{-\bar{y}/\bar{d}}\,\mathrm{d}\bar{y} \\ &= \frac{2}{A_k}(0.09A_k^2 - 1)\{2\bar{d}^3 - \mathrm{e}^{-\bar{y}/\bar{d}}(2\bar{d}^3 + 2\bar{y}\bar{d}^2 + \bar{y}^2\bar{d})\}.\end{aligned} \tag{3.12}$$

The constant $\bar{d}$ will be found by matching to the Clauser viscosity:

$$\nu_\infty = (\epsilon C_{\mathrm{c}})\,U_\infty\,\delta_*, \tag{3.13}$$

where C_{c} is a constant and δ_* is the displacement thickness. The constant in (3.13) is expressed as ϵC_{c} to be consistent with the present asymptotic analysis – that is, this form leads to a systematic balance between inertia, pressure gradient and shear stress gradient in the outer region. Note that with the scaling (2.10), the Clauser model becomes $\tilde{\nu}_{\mathrm{T}} = C_{\mathrm{c}}\tilde{\delta}_*$. It is more usual to equate ϵC_{c} to 0.017. However, here C_{c} will be treated as a model parameter: experiments show quite clearly that ϵC_{c} is not equal to 0.017 in APG boundary layers (Simpson, Chew & Shivaprasad 1981).

Equating the limit of (3.12) as $\bar{y} \to \infty$ to the Clauser viscosity gives

$$\frac{4}{A_k}(0.09A_k^2 - 1)\,\bar{d}^3 = (C_{\mathrm{c}}\tilde{\delta}_*)^2; \tag{3.14}$$

or, $\bar{d} = 1.35(C_c \tilde{\delta}_*)^{\frac{1}{3}}$ with the usual k–ε model constants. $\tilde{\delta}_* = \delta_*/\delta$ is the scaled displacement thickness.

The interpolation formula for C_μ is somewhat arbitrary. A simpler interpolation for $\bar{\nu}_T$ is obtained if $C_\mu = 0.064 + 0.026\,e^{-y^3/d^3}$. Then

$$\bar{\nu}_T^2 = \frac{2}{3A_k}(0.09A_k^2 - 1)\,\bar{d}^3(1 - e^{-y^3/d^3}) \tag{3.15}$$

and $\bar{d} = 2.45(C_c \tilde{\delta}_*)^{\frac{1}{3}}$. In dimensional terms this can be written

$$\nu_T^2 = \nu_\infty^2(1 - e^{-\alpha y^3/\nu_\infty^2 2.45^3}),$$

where ν_∞ is the constant eddy viscosity (3.13) in the outer region. A corresponding interpolation formula for ZPG boundary layers is obtained by replacing the linear stress variation, αy, by the surface stress, u_*^2, and by replacing the constant 2.45^3 with $1/\kappa^2$, where κ is the von Kármán constant. Then

$$\nu_T^2 = \nu_\infty^2(1 - e^{-\kappa^2 u_*^2 y^2/\nu_\infty^2}). \tag{3.16}$$

As $y \to \infty$ this becomes the Clauser viscosity, ν_∞; as $y \to 0$, $\nu_T \to \kappa u_* y$. This interpolation formula agrees quite well with experimental data. The formula (3.12) was used to evaluate the constants required for the computations in §4.3; however, it will be shown that similar results are obtained when (3.15) is used.

4. Expansions, matching and skin friction

The scaling given in §2 suggests how asymptotic expansions can be developed in each of the regions. Boundary conditions are given at the wall ($\hat{U} = 0$ at $\hat{y} = 0$) and in the free stream ($\tilde{U} \to 1$ as $\tilde{y} \to \infty$). Thus, to solve the two-point boundary-value problem for the mean flow, and to determine the skin friction, the expansions in the three regions must be matched in their overlap domains. This procedure is described in the present section.

4.1. *Matched expansions*

Equation (2.5) suggests that in the inner region the mean flow should be expanded as

$$\hat{U} = \hat{U}_0 + \epsilon^2 \hat{U}_1 + \ldots. \tag{4.1}$$

The k–ε model suggests a similar expansion for $\hat{\nu}_T$. The solution to (2.6) for $\hat{U}_0$ is

$$\hat{U}_0 = \int_0^{\hat{y}} \frac{\hat{y} + u_*^2/u_p^2}{1 + \hat{\nu}_{T_0}} \mathrm{d}\hat{y}. \tag{4.2}$$

To match with the middle region, this solution can be rewritten in middle-region variables and expanded for $\epsilon \to 0$ (Van Dyke 1975). Let

$$\hat{C}_u = \int_0^\infty \left\{ \frac{\hat{y} + u_*^2/u_p^2}{1 + \hat{\nu}_{T_0}} - \frac{A_u}{2\hat{y}^{\frac{1}{2}}} \right\} \mathrm{d}\hat{y}. \tag{4.3}$$

Then the asymptotic matching principle is that as $\epsilon \to 0$,

$$\begin{aligned} \bar{U} &\to (u_p/U_\infty \epsilon^{\frac{2}{3}})\,\hat{U}_0(\bar{y} u_p\, \delta \epsilon^{\frac{1}{3}}/\nu) \\ &= \epsilon^{\frac{1}{3}} \hat{U}_0(\bar{y}/\epsilon^{\frac{2}{3}}) \\ &\to A_u \bar{y}^{\frac{1}{2}} + \epsilon^{\frac{1}{3}} \hat{C}_u - \epsilon^{\frac{2}{3}} u_*^2 A_u/(u_p^2 \bar{y}^{\frac{1}{2}}) + O(\epsilon). \end{aligned} \tag{4.4}$$

Note that the inner region is not exponentially thin in the APG boundary layer, whereas it is in ZPG boundary layers.

Equation (4.4) suggests that the middle-region expansion proceeds as

$$\bar{U} = \bar{U}_0 + \epsilon^{\frac{1}{3}}\bar{U}_1 + \epsilon^{\frac{2}{3}}\bar{U}_2 + \ldots, \tag{4.5}$$

with a similar expansion for $\bar{\nu}_T$. Then the middle-region equation (2.8) and (4.4) show that

$$\left.\begin{aligned} \bar{U}_0 &= \int_0^{\bar{y}} \frac{\bar{y}}{\bar{\nu}_{T_0}} \mathrm{d}\bar{y} \\ \bar{U}_1 &= \hat{C}_u - \int_0^{\bar{y}} \bar{y} \frac{\bar{\nu}_{T_1}}{\bar{\nu}_{T_0}^2} \mathrm{d}\bar{y} \\ \bar{U}_2 &= \frac{u_*^2}{u_p^2} \int_0^{\bar{y}} \frac{\mathrm{d}\bar{y}}{\bar{\nu}_{T_0}} - \int_0^{\bar{y}} \bar{y} \left\{ \frac{\bar{\nu}_{T_2}}{\bar{\nu}_{T_0}^2} - \frac{\bar{\nu}_{T_1}^2}{\bar{\nu}_{T_0}^3} \right\} \mathrm{d}\bar{y}. \end{aligned}\right\} \tag{4.6}$$

It will become clear that the middle-region expansion must be carried to $O(\epsilon^{\frac{2}{3}})$ if the friction velocity u_* is to be determined.

The solution (4.6) can be rewritten in outer variables and expanded as $\epsilon \to 0$. Let

$$\bar{C}_u = \int_0^{\infty} \left\{ \frac{\bar{y}}{\bar{\nu}_{T_0}} - \frac{\bar{y}}{\bar{\nu}_{\infty}} \right\} \mathrm{d}\bar{y}, \qquad \hat{C}'_u = \hat{C}_u - \int_0^{\infty} \bar{y} \frac{\bar{\nu}_{T_1}}{\bar{\nu}_{T_0}^2} \mathrm{d}\bar{y}, \tag{4.7}$$

in which $\bar{\nu}_{\infty}$ is the eddy viscosity evaluated as $\bar{y} \to \infty$; in the present case this is equal to $\tilde{\nu}_T$, the constant value determined by the Clauser model. It will be assumed that the integrals converge in the form written. Then, as in (4.4),

$$\begin{aligned} \tilde{U} &\to \epsilon^{\frac{2}{3}} \bar{U}(\tilde{y}/\epsilon^{\frac{1}{3}}) \\ &\to \frac{\tilde{y}^2}{2\bar{\nu}_{\infty}} + \epsilon^{\frac{2}{3}} \bar{C}_u + \epsilon \hat{C}'_u + \epsilon \frac{u_*^2}{u_p^2} \frac{\tilde{y}}{\bar{\nu}_{\infty}} + O(\epsilon^{\frac{4}{3}}). \end{aligned} \tag{4.8}$$

The behaviour of V at large $\bar{y}$ is needed to complete the matching with the outer region. In the middle region $U = U_{\infty} \epsilon^{\frac{2}{3}} \bar{U}(y/\delta\epsilon^{\frac{1}{3}})$. If ϵ – or, in the present context δ/L – is taken as constant, independent of x, then

$$U_{\tilde{x}} = -\epsilon^{\frac{2}{3}} U_{\infty} (\bar{U} + \bar{y}\beta\bar{U}'), \tag{4.9}$$

where $\beta \equiv \delta_{\tilde{x}}/\delta$; the abbreviation β for this parameter is introduced for convenience. If the definition (2.1) of L is substituted into the expression for β it assumes the more familiar dimensional form $\beta = -\delta_x U_{\infty}/\delta U_{\infty x}$. In general (4.9) should contain $\mathrm{d}\ln\epsilon/\mathrm{d}\tilde{x}$ as an additional parameter; but we are simplifying matters by assuming this term to be negligible. (In the self-similar analysis of §4.2 it will be necessary to take ϵ to be constant to a first approximation.)

It follows from (4.9) and the continuity equation (2.4) that to lowest order in ϵ

$$V = -\frac{1}{L} \int_0^y U_{\tilde{x}} \mathrm{d}y = -\epsilon^{\frac{4}{3}} \int_0^{\bar{y}} U_{\tilde{x}} \mathrm{d}\bar{y}$$

in the middle region. Substituting (4.9) gives

$$V = \epsilon^2 U_{\infty} \left[(1-\beta) \int_0^{\bar{y}} \bar{U} \mathrm{d}\bar{y} + \beta\bar{y}\bar{U} \right]. \tag{4.10}$$

As $\bar{y} \to \infty$ this gives

$$\frac{V}{U_\infty \epsilon^2} \to (1+2\beta)\frac{\bar{y}^3}{6\bar{\nu}_\infty} + \bar{C}_u \bar{y} + \bar{C}_v, \tag{4.11}$$

where

$$\bar{C}_v = (1-\beta)\int_0^\infty \left\{\bar{U} - \bar{C}_u - \frac{\bar{y}^2}{2\bar{\nu}_\infty}\right\} \mathrm{d}\bar{y}. \tag{4.12}$$

Expression (4.8) suggests the outer-region expansion

$$\tilde{U} = \tilde{U}_0 + \epsilon^{\frac{1}{3}}\tilde{U}_1 + \epsilon^{\frac{2}{3}}\tilde{U}_2 + \ldots, \tag{4.13}$$

and similarly for $\tilde{V}$. It is assumed that the Clauser model for $\tilde{\nu}_\mathrm{T}$ is valid to all orders. The equation (2.11) for the mean flow in the outer region depends on $\delta_{\tilde{x}}/\delta \equiv \beta$. In order to solve the outer flow β must be expanded as

$$\beta = \beta_0 + \epsilon^{\frac{1}{3}}\beta_1 + \epsilon^{\frac{2}{3}}\beta_2 + \ldots. \tag{4.14}$$

This is necessary because β parametrizes the dependence of u_* on the pressure gradient; in other words, the mean flow equations are being solved for β given u_*, which is a sort of inverse formulation of the skin friction problem. In a formal asymptotic development, the expansions (4.13) and (4.14) must be substituted into

$$\left.\begin{aligned} \tilde{U}\tilde{U}_{\tilde{x}} + \tilde{V}\tilde{U}_{\tilde{y}} - \beta\tilde{y}\tilde{U}\tilde{U}_{\tilde{y}} - \tilde{U}^2 + 1 &= \tilde{\nu}_\mathrm{T}\tilde{U}_{\tilde{y}\tilde{y}}, \\ \tilde{U}_{\tilde{x}} + \tilde{V}_{\tilde{y}} - \tilde{U} - \beta\tilde{y}\tilde{U}_{\tilde{y}} &= 0, \end{aligned}\right\} \tag{4.15}$$

which are the mean momentum and continuity equations in the outer region.

These equations must be solved subject to the matching conditions (4.8). Thus, at $\tilde{y} = 0$:

$$\left.\begin{aligned} \tilde{U}_0 = \tilde{U}_{0_{\tilde{y}}} = 0; \quad \tilde{U}_1 = \tilde{U}_{1_{\tilde{y}}} = 0; \\ \tilde{U}_2 = \bar{C}_u, \quad \tilde{U}_{2_{\tilde{y}}} = 0; \quad \tilde{U}_3 = \hat{C}'_u, \quad \tilde{U}_{3_{\tilde{y}}} = u_*^2/u_p^2\,\bar{\nu}_\infty. \end{aligned}\right\} \tag{4.16}$$

As $\tilde{y} \to \infty$, $\tilde{U}_0 \to 1$ and $\tilde{U}_n \to 0$, $n > 1$. One sees that $\tilde{U}_1 \equiv 0$.

By continuity V is $O(\epsilon^2 U_\infty)$ in the middle region (see (4.11)). Then, by the scaling in (2.10) and the expansion (4.13), $\tilde{V}_3(0) = \bar{C}_v$ where $\bar{C}_v$ is the constant defined in (4.12). All terms in $\tilde{V}$ lower than the third order vanish at $\tilde{y} = 0$.

4.2. *Self-similar case*

Rather than address the full boundary-layer problem posed by (4.15) and (4.16), we will restrict attention to self-similar flow, in the interest of tractability, and for illustrative purposes. The definition of self-similarity is that partial derivatives with respect to $\tilde{x}$ should vanish from (4.15). For strict self-similarity all coefficients in the equations and boundary conditions must be independent of $\tilde{x}$: β, $\tilde{\nu}_\mathrm{T}$, u_*/u_p and ϵ all have to be constant. At lowest order in ϵ, self-similarity only requires that β and $\tilde{\nu}_\mathrm{T}$ be constant, which essentially is the condition usually cited for high-Reynolds-number flow (Clauser 1956). The additional conditions listed are general requirements (Townsend 1976) and not peculiar to the present analysis. The asymptotic approximations of §4.1 would remain valid to the order given if β and $\tilde{\nu}_\mathrm{T}$ were allowed to have $\tilde{x}$-dependence of $o(\epsilon)$, u_*/u_p were allowed to have $\tilde{x}$-dependence of $o(1)$ and ϵ were allowed to have $\tilde{x}$-dependence of $o(\epsilon^{\frac{1}{3}})$. Thus one might also regard the present analysis as an approximation suitable to a slowly varying flow.

Under self-similarity, (4.15) can be simplified by a change of dependent variable. Let $f(\tilde{y})$ be defined by

$$\tilde{U} = f'(\tilde{y}) \tag{4.17}$$

so that f' is equal to the complete non-dimensional velocity, not to only its defect. APG boundary layers have a large wake deficit, so linearization about the free-stream velocity is not justified.

The continuity equation will be satisfied if

$$\tilde{V} = (1-\beta)f + \beta\tilde{y}f'. \tag{4.18}$$

Substituting (4.17) and (4.18) into (4.15) gives

$$(1-\beta)\,ff'' + 1 - f'^2 = \tilde{\nu}_T f'''. \tag{4.19}$$

This must be solved subject to $f'(\infty) = 1$ and conditions (4.16) at $\tilde{y} = 0$.

An equation for β is obtained by integrating (4.19) subject to the boundary condition at infinity:

$$\beta - 1 = \frac{\int_0^\infty \{1-f'^2\}\,\mathrm{d}\tilde{y} + \tilde{\nu}_T f''(0)}{\int_0^\infty ff''\,\mathrm{d}\tilde{y}}. \tag{4.20}$$

The right-hand side of (4.20) is implicitly a function of ϵ and u_*/u_p. Hence (4.20) is the drag law relating skin friction to pressure gradient – at least implicitly.

In a formal development, the self similar function f must be expanded, as $\tilde{U}$ was in (4.13), and substituted into (4.19) along with the expansion (4.14) of β. This leads to the series of problems,

$$\left.\begin{aligned} (1-\beta_0)f_0f_0'' + 1 - f_0'^2 &= \tilde{\nu}_T f_0''', \\ f_1 \equiv 0, \quad \beta_1 &\equiv 0, \\ (1-\beta_0)(f_0f_2'' + f_2f_0'') - 2f_2'f_0' &= \tilde{\nu}_T f_2''' + \beta_2 f_0 f_0'', \\ (1-\beta_0)(f_0f_3'' + f_3f_0'') - 2f_3'f_0' &= \tilde{\nu}_T f_3''' + \beta_3 f_0 f_0''. \end{aligned}\right\} \tag{4.21}$$

Strictly, if $\tilde{\nu}_T$ depends on δ_*/δ as in (3.13) it too should be expanded; for simplicity, this was not done in (4.21). The boundary conditions which follow from (4.16) are

$$\left.\begin{aligned} f_0(0) = f_0'(0) = f_0''(0) = 0, \quad f_0'(\infty) &= 1; \\ f_2(0) = f_2''(0) = f_2'(\infty) = 0, \quad f_2'(0) &= \bar{C}_u; \\ f_3(0) = \frac{\bar{C}_v}{1-\beta_0}, \quad f_3'(0) = \hat{C}_u', \quad f_3''(0) = \frac{u_*^2}{u_p^2\,\bar{\nu}_\infty}, \quad f_3'(\infty) &= 0 \end{aligned}\right\} \tag{4.22}$$

(recall that $\bar{\nu}_\infty = \tilde{\nu}_T = C_c\,\tilde{\delta}_*$). These boundary conditions to (4.21) determine both f and β.

At lowest order, from (4.17), (4.21) and (4.22),

$$\beta_0 = 3 + \frac{\chi}{1-\chi},$$

where

$$\chi = \int_0^\infty (1-\tilde{U})^2\,\mathrm{d}\tilde{y} \Big/ \int_0^\infty (1-\tilde{U})\,\mathrm{d}\tilde{y}.$$

This was derived in the same manner as (4.20). If $0 \leqslant \tilde{U} \leqslant 1$ for all $\tilde{y}$, then

$$0 < \chi < 1$$

and $\beta_0 > 3$. Thus, a self-similar solution (without flow reversal) is only possible if

$a \equiv -1/\beta > -\frac{1}{3}$. An asymptotic analysis of (4.19) shows that if $\beta \geqslant 3$, the solution with bounded displacement thickness behaves like

$$f' \to 1 + O(\mathrm{e}^{(1-\beta)y^2/2\bar{\nu}_\mathrm{T}}/y^{(\beta-3)/(\beta-1)}) \quad \text{as} \quad \tilde{y} \to \infty.$$

Thus, the convergence to uniform flow at infinity is exponentially fast. This observation was help in the numerical analysis.

4.3. *Numerical solution*

It is convenient for numerical purposes to change the independent variable in (4.19) to $z = y/\tilde{\nu}_\mathrm{T}^{\frac{1}{2}}$ and to introduce the dependent variable $H(z) = (f - \tilde{y})/\tilde{\nu}_\mathrm{T}^{\frac{1}{2}}$. Equation (4.19) then becomes

$$(1-\beta)(H+z)H'' - (2+H')H' = H'''. \tag{4.23}$$

Boundary conditions to (4.23) follow from (4.22) and the definition of H:

$$\left.\begin{aligned} H(0) &= \frac{\epsilon \bar{C}_v}{\tilde{\nu}_\mathrm{T}^{\frac{1}{2}}(1-\beta)}; \quad H'(0) = -1 + \epsilon^{\frac{2}{3}}\bar{C}_u + \epsilon \hat{C}'_u; \\ H''(0) &= \frac{\epsilon u_*^2}{\tilde{\nu}_\mathrm{T}^{\frac{1}{2}} u_P^2}; \quad H'(\infty) = 0. \end{aligned}\right\} \tag{4.24}$$

Rather than formally expanding the solution, we regard the above problem as an approximation for small but finite ϵ; thus, in the present section we are using a consistent small-ϵ approximation, but not evaluating a formal asymptotic series. This is done for reasons which will become clear as the numerical results are presented.

The normalized displacement thickness

$$\frac{\delta_*}{\delta} = \int_0^\infty \left\{1 - \frac{U}{U_\infty}\right\} \mathrm{d}\tilde{y}$$

is equal to $-\tilde{\nu}_\mathrm{T}^{\frac{1}{2}} H(\infty)$. Hence, the Clauser viscosity (3.13) becomes

$$\tilde{\nu}_\mathrm{T} = \bar{\nu}_\infty = (C_\mathrm{c} H(\infty))^2. \tag{4.25}$$

The Clauser constant C_c is regarded as an empirical constant of the flow. In the numerical computations (4.25) was substituted into the boundary conditions (4.24).

Before (4.23) can be integrated numerically, values of the constants in (4.24) are needed. For the barred constants, the interpolation formula (3.12) was used. Evaluating the integrals in (4.7) and (4.12) numerically gives

$$\bar{C}_u = 10.0\frac{\bar{d}^2}{\bar{\nu}_\infty}, \quad \bar{C}_v = 15.9(\beta-1)\frac{\bar{d}^3}{\bar{\nu}_\infty}; \tag{4.26}$$

$\bar{d}$ is given by (3.14) with (4.25):

$$\bar{d} = 1.35(C_\mathrm{c} H(\infty))^{\frac{4}{3}}.$$

It is assumed that no first-order correction to $\bar{\nu}_\mathrm{T}$ is needed, so that $\hat{C}'_u$ is equal to $\hat{C}_u$ (see (4.7)). $\hat{C}_u$ is evaluated using equation (5.15.3) of Townsend (1976). In the present context, that equation behaves as

$$\hat{U} \to A_u\left(\hat{y}^{\frac{1}{2}} - \frac{u_*}{u_p}\right) + \frac{u_*}{\kappa u_p}\left(\ln\left[\frac{4u_*^3}{u_p^3}\right] + B\right) \quad \text{as} \quad \hat{y} \to \infty.$$

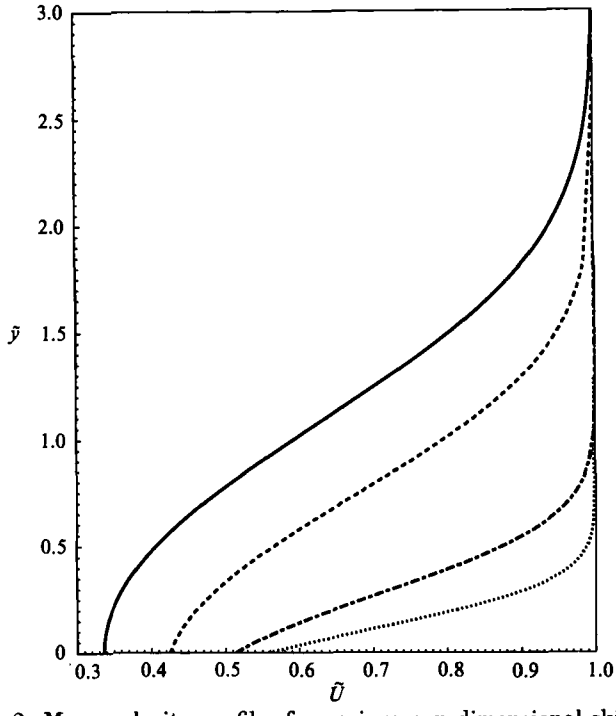

FIGURE 2. Mean velocity profiles for various non-dimensional skin frictions: ——, $u_*/u_p = 0$; – – –, 5; —·—, 9; · · · · ·, 10.

Substituting the standard (ZPG) values of $\kappa = 0.4$, $B/\kappa = 5.0$ and the present value of $A_n = 7.65$ gives

$$\hat{C}_u = 0.82\frac{u_*}{u_p} + 7.5\frac{u_*}{u_p}\ln\frac{u_*}{u_p}. \tag{4.27}$$

The value of B is most likely influenced by pressure gradient, so (4.27) is probably unsuitable when the pressure gradient times δ_* is large compared to the skin friction. In fact, this formulation for $\hat{C}_u$ is not likely to be appropriate when $u_*/u_p \to 0$ because (4.27) is not analytic at zero surface stress – u_* is defined as the square root of the surface stress. Also, the logarithmic formula used in (4.27) is not likely to be valid when u_* becomes very small. As was mentioned previously, a more suitable treatment of the wall layer might make use of a closure model; but such an elaboration is well beyond the scope of the present paper.

4.4. *Results*

A fourth-order Runge–Kutta shooting method was used to solve (4.23) with (4.24) numerically. Some results are shown in figures 2–4. Figure 2 shows profiles of the mean velocity with $C_c = 1.7$ and $\epsilon = 0.002$ and for various values of u_*/u_p. Because the numerical constants in (4.26) are relatively large, ϵ is required to be quite small. The figure shows how the wake fills in as the friction velocity is increased. The displacement thickness is reduced thereby, so the Clauser viscosity decreases as the friction velocity increases.

Figure 3 shows how β varies with surface stress τ_w, normalized here as $\epsilon\tau_w/u_p^2$, where $\tau_w = u_*^2$; $\epsilon\tau_w/u_p^2$ is a natural quantity to plot on the abscissa because it appears in the boundary condition (4.24). The numerical values on the abscissa are small, since u_*/u_p is of order unity; the axis extends to values of this ratio equal to about

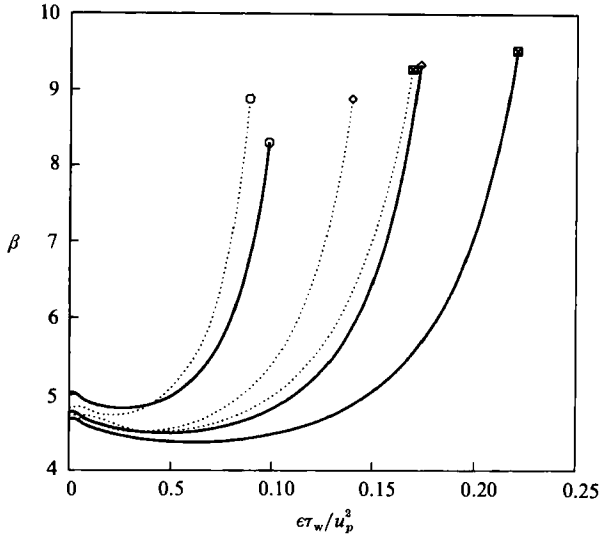

FIGURE 3. Dependence of β on skin friction. $\epsilon = 0.002$ (——), 0.004 (· · · · ·): ○, $C_c = 0.4$; ◇, 1.0; ⊠, 1.7.

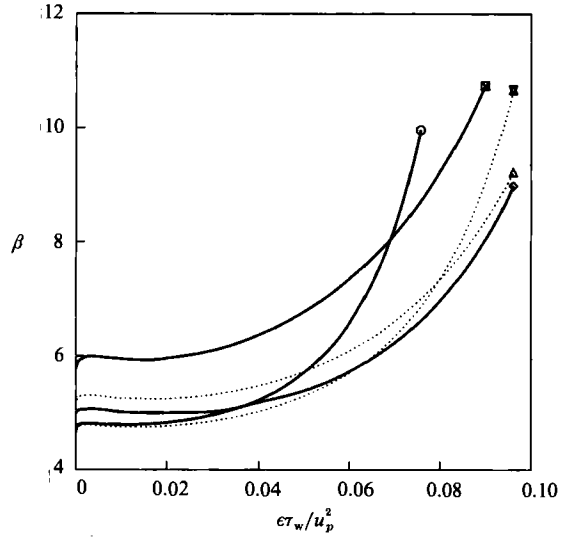

FIGURE 4. Dependence of β on skin friction for $\epsilon = 0.01$: ○, $C_c = 0.4$; ×, 0.7; ◇, 1.0; △, 1.3; ⊠, 1.7.

10. Curves are plotted with $\epsilon = 0.004$ and 0.002, for the values of C_c indicated. Figure 4 contains similar curves for $\epsilon = 0.01$. This figure includes the commonly used value of the Clauser constant $\epsilon C_c = 0.017$. The dependence of β on C_c is quite different from that in figure 3; but its dependence on τ_w is qualitatively similar.

β is defined as $-\delta' U/U'\delta$, so it is inversely proportional to the adverse pressure gradient. In figures 3 and 4, at large surface stress the skin friction decreases as the pressure gradient becomes increasingly adverse; i.e. as β decreases. This behaviour might be expected. However, as τ_w increases from zero, there is a range of τ_w within which β decreases before increasing at large τ_w; so the solution for τ_w at given β is double valued in a very small range of β. The decrease of β at small surface stress might be rationalized by attributing it to a decrease of δ' as τ_w increases from 0: δ'

appears in the numerator of β so this decreases β. One expects more rapid growth of δ as a boundary layer approaches a point of zero mean skin friction. However, it should be recognized that the present solution is for a self-similar, equilibrium layer, so it is not entirely appropriate to interpret figure 3 in terms of a layer approaching a point of vanishing skin friction.

The mathematical source of the initial decrease of β with increasing τ_w is as follows. Equations (4.23) and (4.24) show that β depends on ϵ and u_* through only the boundary conditions; thus

$$\beta = F(H(0), H'(0), H''(0)).$$

This relation can be differentiated and evaluated at $(0, -1, 0)$ to find the limiting behaviour when $\epsilon \to 0$. The derivatives were computed numerically. The derivatives with respect to the first, second and third arguments were found to be $\partial_1 F = -21.3$, $\partial_2 F = -14.1$ and $\partial_3 F = 0.0$ at $(0, -1, 0)$. Also $F(0, -1, 0) = 6.029$. We were unable to prove that $\partial_3 F(0, -1, 0) = 0$, the result cited is entirely numerical: an analysis of a linearized version of (4.23) gave a non-zero value for this derivative; the numerical value of 0 would seem to be a consequence of the nonlinear advective derivative vanishing at $\tilde{y} = 0$.

The dependence of β on u_* is entirely through the $O(\epsilon)$ terms in the second and third arguments of F. However, at $(0, -1, 0)$, F becomes insensitive to its third argument. Hence β decreases with increasing τ_w (when $u_*/u_p > 0.9$) because $\hat{C}_u$ increases with u_* and the derivative of F with respect to its second argument is negative. When $u_*/u_p < 0.9$ there is a slight increase of β with u_* because $\hat{C}_u$ becomes negative initially (see (4.27)). This initial increase becomes more pronounced as ϵ increases, as seen in figure 4; however, it should again be emphasized that (4.27) is unlikely to be valid as $u_* \to 0$. Although the detailed behaviour of β is a consequence of the formula used for $\hat{C}_u$, the values for derivatives of F are a property of (4.23), which is essentially the Falkner–Skan equation. The only modelling involved in that equation is the assumption of a constant eddy viscosity in the outer region. Thus, the decrease of β with increasing u_* will occur with any model for which $\hat{C}_u$ increases with u_*. Assuming that β ultimately increases, the solution inevitably will be double valued.

The rapid increase of β at large τ_w is a consequence of the boundary condition on H''. This observation was made first in the solution to a linearized version of (4.23), and then confirmed by numerical computations with $H''(0)$ set to zero. When $H''(0)$ was set to zero, β continued to decrease with increasing u_*, instead of turning up sharply as it does in the figures. In the light of previous paragraphs, it is clear that for $H''(0)$ to have an effect on β the boundary conditions must differ from $(0, -1, 0)$. Although this might at first seem to be inconsistent with the small-ϵ approximation, it can be seen that the outer problem remains unchanged as long as $\epsilon u_*^2/u_p^2$ is $O(\epsilon^p)$ for any $p > 0$. As long as this condition is satisfied, an outer region can be distinguished asymptotically (see the reasoning behind (2.14)). The present problem then remains appropriate even when u_* becomes large, provided $\epsilon u_*^2/u_p^2$ is small, as it is in figures 3 and 4.

In order to assess the sensitivity of our results to the interpolation formula for $\bar{\nu}_T$, the constants in (4.26) were re-evaluated using (3.15). This gives

$$\bar{C}_u = 1.64 \frac{\bar{d}^2}{\bar{\nu}_\infty}, \quad \bar{C}_v = 0.462(\beta - 1) \frac{\bar{d}^3}{\bar{\nu}_\infty}, \tag{4.28}$$

with $\bar{d} = 2.45(C_c H(\infty))^{\frac{1}{3}}$. The constants in these expressions for $\bar{C}_u$ and $\bar{C}_v$ are considerably smaller than previously, although much of the decrease is counteracted

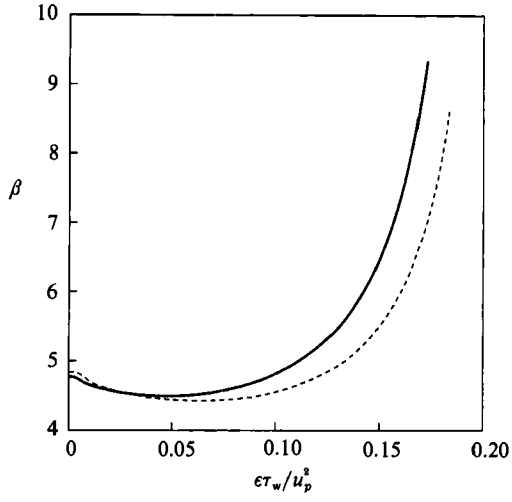

FIGURE 5. Comparison of results for two interpolation formulae for $\epsilon = 0.002$, $C_\epsilon = 1.0$: ——, (3.12); – – –, (3.15).

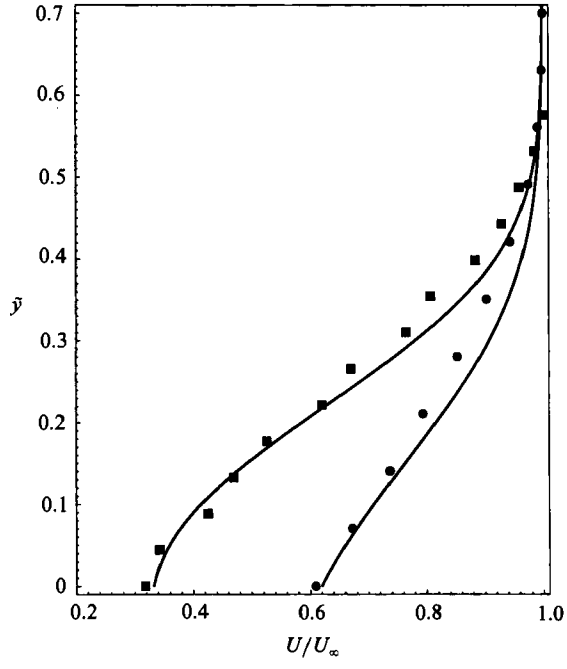

FIGURE 6. Comparison of computations (——) to experimental data on self-similar APG boundary layers. Data from Coles & Hirst (1968): ●, Bradshaw & Ferris; ■, Stratford.

by the increase in $\bar{d}$. Figure 5 shows computations using (4.28) compared to those using (4.26). The qualitative behaviour is very similar in the two cases.

Computations were done with $\epsilon = 0.005$ and $u_*/u_p = 5.0$, and with $\epsilon = 0.007$ and $u_*/u_p = 1.6$, corresponding respectively to experimental self-similar APG boundary layers measured by Bradshaw & Ferris, and by Stratford (Coles & Hirst 1968). The former experiment is that shown by figure 1. Those experimental data points which lay in the outer region are plotted in figure 6, along with computed curves. The outer region of the experiments was demarcated by the top of the half-power layer, which

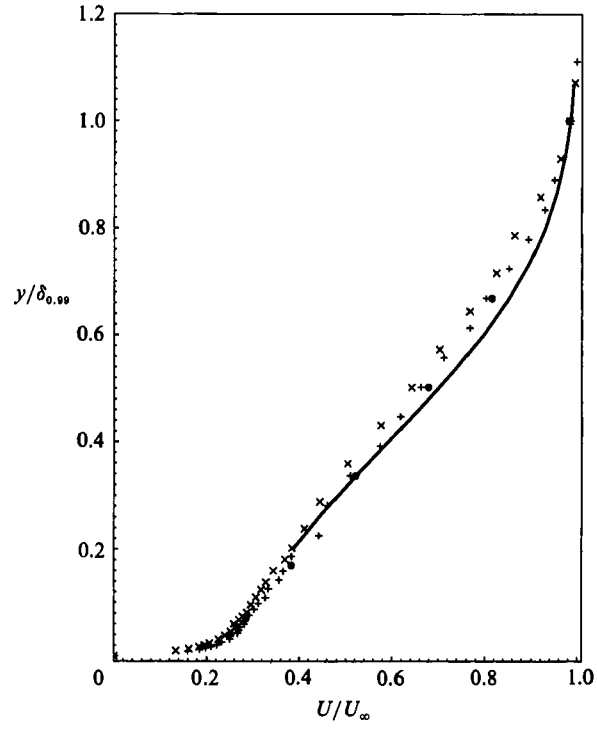

FIGURE 7. Comparison of computations (——) to experiment by Driver (1991): ×, $x = 152$ mm; ●, 228 mm; +, 304 mm.

can be determined from plots like those of Schofield (1981, figure 5). The y-coordinate of the data was arbitrarily scaled so that the last experimental point fell on the computed curve; this amounts to normalizing y by the 99% boundary-layer thickness. C_c was adjusted so that the computation agreed reasonably well with the lowest data point. The values of C_c were 1.5 for the Bradshaw data and 0.4 for the Stratford data. The primary purpose of figure 6 is to show that reasonable agreement can be achieved with the experimental profiles. A further point of agreement is that Stratford's boundary layer has $1/\beta = 0.23$, while our computation gave $1/\beta = 0.21$. A point of disagreement is that Bradshaw's layer has $1/\beta = 0.255$ while our computation gave $1/\beta = 0.15$. Indeed, with the constants (4.26) we did not obtain values of $1/\beta$ as high as 0.255 in any of our computations. This could very likely reflect the coarseness of the present turbulence modelling.

In figure 7 data from Driver (1991) is shown along with a computation of a wake-region profile. This computation had $\epsilon = 0.005$ and $u_*/u_p = 3.66$, corresponding to the experiment, and C_c was set to 0.34. In the figure data are shown all the way to the wall so that the relative location of the outer region can be seen. The computed curve extends only through the wake portion of the data, where it is valid. Driver's experiment was not designed to produce self-similar flow. We have selected data from his case B, which does not separate, in a downstream region where the profiles become approximately self-similar.

4.5. *Discussion*

When the results shown in figures 3 and 4 were obtained, we were at first disconcerted to find that β decreased with increasing u_* over a range of surface stress, and that u_* was a double-valued function of β. We subsequently found that this behaviour

had been noticed some time ago by Clauser (1954); he had found experimental evidence that two self-similar turbulent boundary layers might exist for a given APG. He reached this conclusion through a semi-empirical evaluation of the integrated momentum balance, using his wind tunnel data for equilibrium boundary layers. More recent analyses, also based on semi-empirical evaluations of the integrated momentum balance, concur with Clauser's original conclusion (Townsend 1976; Schofield 1981). It is remarkable that we have been led to the same result through a very different sort of analysis. Our figure 3 bears a striking similarity to Clauser's figure 26 – the quantities plotted on his axes are inverse to ours; thus, his horizontal axis is proportional to $1/\tau_w$ and his vertical axis is $1/\beta$. Clauser observed that the two boundary layers which exist in a small range of β correspond to flows either with a large momentum deficit, having small skin friction, or with a small deficit, and being near to a ZPG boundary layer. In the former case the downstream increase of the momentum thickness is balanced largely by pressure forces, while in the latter it is balanced primarily by skin friction. Thus, the two equilibrium layers are distinguished by how prominent a role the pressure gradient plays.

As is frequently remarked, the conditions for self-similarity require that δ grows linearly with x, and that U_∞ varies with a negative power of x (Townsend 1976): in the present notation the required power-law dependence is $U_\infty \sim x^{-1/\beta}$. The Stratford, zero-stress equilibrium boundary layer has $1/\beta = 0.23$ and Clauser (1954) suggested that in his experiments the largest value for which a non-separating equilibrium boundary layer might be produced was $1/\beta = 0.29$. In the present analysis the value of β at zero skin friction depends on ϵ and C_c, but it agrees in order of magnitude with these experimental values; for instance, in figure 3 at $\tau_w = 0$, $1/\beta$ lies between 0.20 and 0.22. When $\epsilon = 0.002$ and $C_c = 1.7$ the maximum value of $1/\beta$ is 0.23. Thus, despite the fairly crude modelling, the results of our analysis seem reasonable.

The dependence of β on τ_w when τ_w is small is determined by the boundary condition on H', as was explained in §4.3. This boundary condition was derived by asymptotic matching between the outer, middle and inner regions. The asymptotic matching is essential to our analysis. It is also essential that the fully nonlinear Falkner–Skan equation was solved. An analysis (not presented here) of a linearized version of that equation resulted in the τ_w-dependence of β being determined by the boundary condition on H'', with the consequence that β was single valued, and increased linearly with τ_w. The numerical results are so drastically different as to make the linearized analysis useless.

It should be remarked that our analysis bears some similarity to one presented in Townsend (1976). However, Townsend simply patched together assumed velocity profiles in the wall and wake regions. He did not insist that they merge smoothly, as is done by asymptotic matching; therefore, he did not recognize that the wall and wake regions of strong APG boundary layers do not match. Thus there is a rather substantial formal difference between the present development and Townsend's. In the wake region Townsend noted that Clauser's eddy viscosity model led to the Falkner–Skan equation, but Townsend did not solve this equation; rather, he adopted a shape model which is a linear combination of solutions to the linearized Falkner–Skan equation. We have noted above that the linearized equation does not give even qualitatively correct results. Thus, one can have little confidence in the development described by Townsend. Nevertheless, it should duly be noted that Townsend recognized that there are many significant differences between APG and ZPG boundary layers, such as the large wake deficit in the former, and these insights guided his analysis.

The solution to the matching problem described here gives the skin friction law for APG boundary layers. However, that solution had to be obtained numerically. This is rather different from the logarithmic law which exists for ZPG boundary layers: that law contains a constant which must be determined by experiment or by modelling, but the basic logarithmic dependence can be deduced from the asymptotic scaling alone (Mellor 1972).

Some previous investigators have assumed that the ZPG friction law applies up to separation (Melnik 1989). A consequence of this assumption is that the 'slip velocity' in the outer region ($f'(0)$ in the present case) must vanish when the skin friction vanishes. However, the experimental evidence is quite strong that a $y^{\frac{1}{2}}$ region forms in the APG boundary layer prior to the skin friction vanishing (Schofield 1981). This means that the present structure will exist upstream of a turbulent separation. One sees in (4.22) and (4.24) that the middle region produces a slip velocity of $O(\epsilon^{\frac{3}{8}})$ in the outer region, while the skin friction does not enter until $O(\epsilon)$. Thus, there is no obvious reason for the slip velocity to vanish with the skin friction. This observation is significant to the issue of whether a Goldstein type of singularity is associated with turbulent separation (Melnik 1989, 1991; of course, it is not clear that a mean flow eddy viscosity model can elucidate the structure of turbulent separation). Only the outer region is nonlinear, so any movable singularity must occur in that region. If the slip velocity is not zero when the skin friction vanishes then flow reversal in the nonlinear region will not occur at a point of zero wall stress. Thus, the nature of the breakdown of the turbulent-boundary-layer approximation at separation remains to be clarified.

It should be appreciated that the self-similar solutions presented here do not apply directly to separating flow; the full problem (4.15) and (4.16) must be solved. The limit $u_* \to 0$ in the self-similar solution corresponds to the Stratford, zero-stress turbulent boundary layer (Perry & Schofield 1973), and not to a boundary layer with a point of zero skin friction.

Because a turbulent boundary layer can withstand a large adverse pressure gradient, it can develop a large velocity defect without mean flow reversal. That leads to the substantial changes in scaling and in turbulence structure which have been discussed in the present paper.

REFERENCES

BRADSHAW, P. 1967 Equilibrium turbulent boundary layers. *J. Fluid Mech.* **29**, 625–646.

BUSH, W. B. & FENDELL, F. E. 1972 Asymptotic analysis of turbulent channel and boundary-layer flow. *J. Fluid Mech.* **56**, 657–681.

CLAUSER, F. H. 1954 Turbulent boundary layers in adverse pressure gradients. *J. Aeronaut. Sci.* **21**, 91–108.

CLAUSER, F. H. 1956 The turbulent boundary layer. *Adv. Appl. Mech.* **4**, 1–51.

COLES, D. E. & HIRST, E. A. (ED.) 1968 *Computation of Turbulent Boundary Layers, AFOSR-IFP-Stanford Conference.*

DRIVER, D. M. 1991 Reynolds shear stress measurements in a separated boundary layer flow. *AIAA Paper* 91-1787.

DURBIN, P. A. 1991 Near wall turbulence closure modelling without 'damping functions'. *Theor. Comput. Fluid Dyn.* **3**, 1–13.

MCDONALD, H. 1969 The effect of pressure gradient on the law of the wall in turbulent flow. *J. Fluid Mech.* **35**, 311–336.

MELLOR, G. L. 1972 The large Reynolds number asymptotic theory of turbulent boundary layers. *Intl J. Engng Sci.* **10**, 851–873.

MELNIK, R. E. 1989 An asymptotic theory of turbulent separation. *Computers Fluids* **17**, 165–184.

MELNIK, R. E. 1991 Some applications of asymptotic theory to turbulent flow. *AIAA Paper* 91-0220.

PATEL, V. C., RODI, W. & SCHEURER, G. 1985 Turbulence models for near-wall and low Reynolds number flows: a review. *AIAA J.* **23**, 1308–1319.

PERRY, A. E. & SCHOFIELD, W. H. 1973 Mean velocity and shear stress distributions in turbulent boundary layers. *Phys. Fluids* **16**, 2068–2074.

SCHOFIELD, W. H. 1981 Equilibrium boundary layers in moderate to strong adverse pressure gradient. *J. Fluid Mech.* **113**, 91–122.

SIMPSON, R. L., CHEW, Y. T. & SHIVAPRASAD, B. G. 1981 The structure of a separating boundary layer. Part 1. Mean flow and Reynolds stresses. *J. Fluid Mech.* **113**, 23–51.

TOWNSEND, A. A. 1976 *The Structure of Turbulent Shear Flows*. Cambridge University Press.

VAN DYKE, M. 1975 *Perturbation Methods in Fluid Mechanics*. Parabolic Press.

YAGLOM, A. M. 1979 Similarity laws for constant-pressure and pressure-gradient turbulent wall flows. *Ann. Rev. Fluid Mech.* **11**, 505–540.

YAJNIK, K. S. 1970 Asymptotic theory of turbulent shear flows. *J. Fluid Mech.* **42**, 411–427.